AN UNSTEADY FLOW STRUCTURE ON THE HEATED ROTATING DISK UNDER THE MIXED CONVECTION CONDITION

Noriyuki FURUICHI*, Masashige YOSHIDA**, Masaya KUMADA**

*National Institute of Advanced Industrial Science and Technology
Center 3, Umezono1-1-1, Tsukuba 305-8563, Japan, E-mail: furuichi.noriyuki@aist.go.jp
**Gifu Univ. Dep. Mechanical and System Engineering
1-1 Yanagido, 501-1193, Japan, E-mail: kumada@cc.gifu-u.ac.jp

ABSTRACT

The flow field under a mixed convection on the heated rotating disk has been measured using ultrasonic velocity profiler (UVP). The measured velocity field is a spatio-temporal one as a function of a radial coordinate and time. The objective of this paper is to clarify a vortex structure caused by instability between the buoyancy and centrifugal force. The vortex appears under typical Reynolds numbers and Grashof numbers and it moves toward outside of the disk. This behavior can be classified into two patterns. The size of the vortex structure decreases with increase in Reynolds number and increases with Grashof number. The traveling velocity of the vortex increases with Grashof number and decreases with increase in Reynolds number in spite of increase of centrifugal force. According of these results, the region dominated by natural, forced and mixed convection is classified in the relationship between Reynolds and Grashof number.

Key words : Mixed convection, Heated rotating disk, UVP, Buoyancy, Centrifugal force

INTRODUCTION

A heated rotating disk can be seen in many industrial applications such as CVD method for a thin film making and a rotor in a gas-turbine and so on. In this flow field, flow direction induced by rotating of the disk is different with one induced by buoyancy. As the basic flow field to consider a heat transfer mechanism under mixed convection, many investigations have been carried out for time-averageed characteristics[1][2].

On the other hand, the flow field behaves a characteristic unsteady structure due to an instability between a natural and forced convection[3][4]. As concerning with that instability, we make attention to a vortex structure which appears on the disk[5]. This vortex can be observed on the critical Grashof number ($Gr_c \sim Re_\omega^{3/2}$) even if the rotating Reynolds number is small as a laminar condition. From a visualization, it was found as a longitudinal vortex stretching to the azimuthal direction. It was also found that the vortex travels to the azimuthal direction due to Coriolis force and to the outside of the disk due to centrifugal force.

To obtain a knowledge of this vortex structure such as an origin of appearance, deformation and traveling path is very important to clarify the unsteady structure of the mixed convection. However, since an experimental investigation is difficult because of the heating and rotating flow field, these structure have not been clarified well. The objective of this paper is to clarify the basic structure of the vortex and the classification of the natural and forced convection based on the rotating Reynolds number and Grashof number.

EXPERIMENTAL METHOD

Experimental apparatus is shown in Fig.1. A radius of the rotating disk submerged in the water tank ($620 \times 720 \times 400$mm) is R=85mm. The water has 400mm depth and free surface condition. To avoid natural convection induced by a temperature difference between the water and ambient air, the water tank is covered by insulators. The rotating disk is consisting of a cupper plate with 5mm thickness and an insulator. Heating was carried out by a heater attached to the cupper plate by an adhesives with high thermal conductivity.

Rotating velocity of the disk was varied 5~25[rpm] (Reynolds number is $Re_\omega = R^2\omega/\nu = 0.66 \times 10^4 \sim 3.29 \times 10^4$). This is laminar condition in un-heating case. A difference of the temperature between the surface of the rotating disk and the water was varied Δt=2.5~55[°C] (Grashof number is $Gr = g\beta(T_w - T_\infty)R^3/\nu = 0.23 \times 10^8 \sim 5.07 \times 10^8$). The temperature of the water is set to T_∞=40[°C] to eliminate a change of an ultrasonic velocity. In the temperature range of 40 ~ 95[°C], the change of the ultrasonic velocity is less than 1%.

A detail of the test section on the heated rotating disk is shown in Fig.2. Measurement was carried out using ultrasonic velocity profiler. A transducer directed to the center of the disk was set outside of it, therefore, measuring component is $v_r(r,t)$ in this experiment. A center line of the transducer is set to z=1.5[mm] upside from the surface of the disk. A basic frequency of the transducer is 8[MHz] and a pulse number is 6. A spatial interval for each measuring point is 0.77[mm] and a time interval for each profile is 41[msec]. Nylon powder (density 1.02, diameter 100[μm]) is mixed to the water as a tracer.

RESULTS AND DISCUSSION

Spatio-Temporal Velocity Field

Typical spatio-temporal velocity field $v_r(r,t)$ is shown in Fig.3 to observe a change of a behavior with Grashof number. The horizontal axis is time and the vertical axis is radius position. In figure (a) which is the case of the largest angular velocity, the velocity component increases with radius position toward the outside of the disk. This obviously indicates an increase of the centrifugal force. Any effect of the heating can not be observed in this figure since a effect of the forced convection is lager than the natural convection. On the other hand, in the figure (b) and (c), some instability can be observed like a stripe structure as indicated by the dotted line. These stripe-like structures angled to right-up show a behavior that some eddy is moving to outside of the disk. Ogino et.al[5] indicated that a vortex structure of crurve like shape caused by the instability of buoyancy appears under typical condition between rotating Reynolds number and Grashof number. They also showed that it moves azimuthal direction with slower than the rotating speed of the disk and moves toward outside of the disk. From a visualization of the flow field under same condition, the vortex structure moving toward the outside of the disk can be also observed in this experiment. The vortex shows up-wash flow by the heating. We can conclude that the stripe structure in the figure shows a vortex moving toward outside.

The vortex structure can be also observed under the figure (c) condition, however, there are some difference behavior between in (b) and (c). In the (b), the appearance point of a vortex is roughly rigid; around $r/R=0.5$, on the other hand in the (c), it is unstable as some reaches to the center of the disk. In the (c), a reverse flow directed to the center of the disk can be observed. This flow is considered an appearance of the natural convection. The flow toward the center can be observed more clearly in the figure (d) which is the largest Grashof number case. In the (d), the vortex toward the outside of the disk can not be observed.

Cross Correlation of Reconstructed Velocity Field

We consider a detail structure of the vortex moving toward the outside of the disk by a cross-correlation of velocity fluctuation. However, the cross correlation coefficient obtained by this computation is strongly affected by the flow toward the center of the disk, especially under a condition dominated by the natural convection. To eliminate of this effect, we compute the two-dimensional Fourier transform as a following formula at first.

$$S(f,k) = \int_{-\infty}^{\infty} \int_{-\infty}^{\infty} v_r(r,t)e^{-ift}e^{-ikr}dtdr \qquad (1)$$

Where, f is frequency and k is wave number. The obtained spectrum $S(f,k)$ phase indicates each energy of the velocity fluctuation toward the outside and the center of the disk separately. To obtain only the velocity fluctuation toward the outside, the phase indicating toward the center was cancelled through a filter. After this computation, the velocity field was reconstructed by a inverse Fourier transform. Typical reconstructed velocity field is shown in Fig.4 corresponding to the Fig.3(c). It can be observed that the velocity component toward the outside of the disk is extracted clearly.
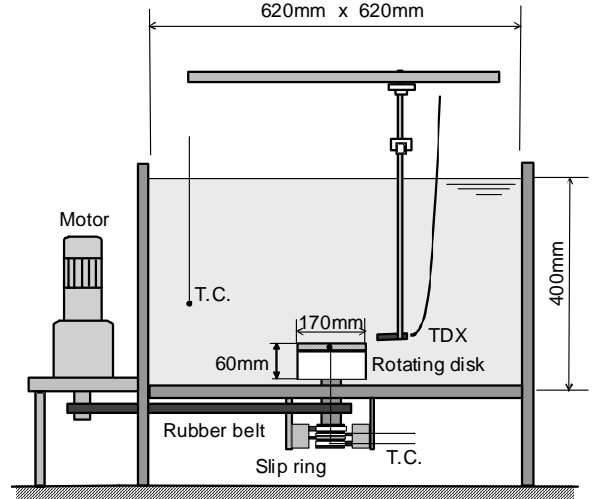

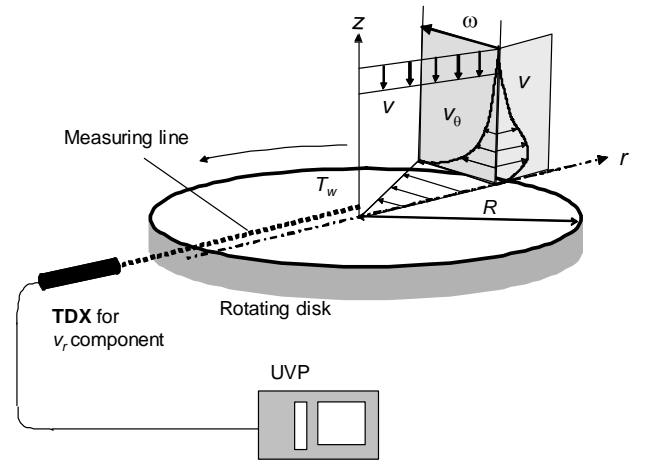Fig.1 Schematic of the experimental apparatus
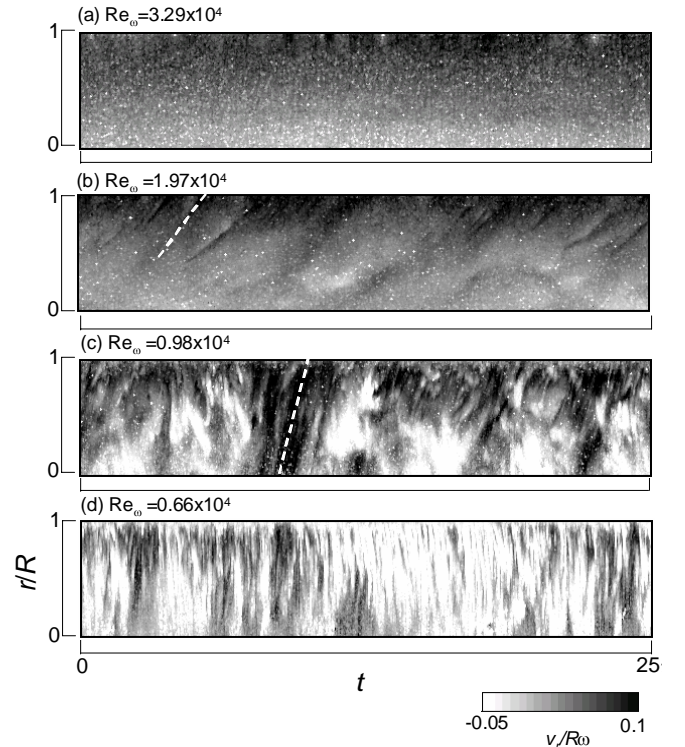

Fig.2 Coordinate system and measuring system

Fig.3 Examples of spatio-temporal velocity field $v_r(r,t)$ at Gr=1.84×10^8

The cross correlation coefficient was computed using the reconstructed velocity field as a following formula.

$$R_{vv}(r_1, r, \tau) = \frac{\overline{v_r^{*'}(r_1,t) \cdot v_r^{*'}(r,t+\tau)}}{\sqrt{\overline{v_r^{*'2}(r_1,t)}} \sqrt{\overline{v_r^{*'2}(r,t+\tau)}}} \qquad (2)$$

Where, r_1 is a fixed point, v_r^* is the reconstructed velocity field by the two-dimensional Fourier transform.

Example of a lag-time and radius position contour map of the correlation coefficient is shown in Fig.5. The fixed point is $r_1 = 0.75R$. The horizontal axis is dimensionless lag-time and the real time scale is same between two maps. The bold line is shown for larger correlation coefficient than 0.3 as a high correlation area. The high correlation area around the lag-time 0 and the fixed point r_1 shows right-up shape because the velocity fluctuation caused by vortex moves toward outside. The shape of the high correlation area in the dimensionless axis is almost same between two maps however the size of (a) for the radius direction is smaller than (b).

To quantitative analysis of the size of vortex, a variation of a integral scale (L_r) at $\tau\omega = 0$ is shown in Fig.6. It is clearly found that the integral scale becomes smaller with increasing Reynolds number. Considered the conservation of an angular momentum, this result shows that the vortex is stretching to the angular direction with increasing Reynolds number. Moreover, the length scale approaches to the zero with Reynolds number. This shows that there is a limitation for an appearance of the vortex toward higher Reynolds number. On the other hand, it can be also found that the integral scale increases with Grashof number. It is considered that the up-wash flow becomes larger with increasing the temperature of the disk.

Traveling Velocity of Vortex

The dotted line in Fig.5 means the most clear ridge line of the contour map. The angle of it indicates that an averaged traveling velocity of velocity fluctuation; in other words vortex toward the outside of the disk. Ogino et al.[5] shows that the traveling velocity of vortex computed by the temperature correlation is almost uniform and it has no correlation with the radius position and Grashof number. However, our investigation as shown the dotted line in the correlation map of Fig.5 is not agreement with that result.

A radial variation of the traveling velocity (v_t) of vortex estimated by the inclination angle of the dotted line in Fig.5 is shown in Fig.7. Obviously, a large difference can be found between the Reynolds number $Re_\omega = 1.34 \times 10^4$ and 1.97×10^4. At the smaller case, the traveling velocity is uniform till $r/R \approx 0.8$. At near of the edge of the disk, it decreases with position because of an interaction between the flow on the disk and of the ambient. On the other hand, the large Reynolds number case, the traveling velocity increases with the radius position.

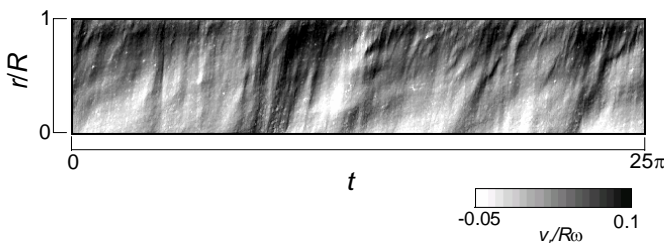In Fig.8, the relationship between the traveling velocity and

the rotating Reynolds number under several Grashof number. This result shows the traveling velocity at $r/R = 0.75$. It is found that the traveling velocity increases with Grashof number. This is caused by a change of the density of the working fluid by heating. On the other hand, when Grashof number is same case
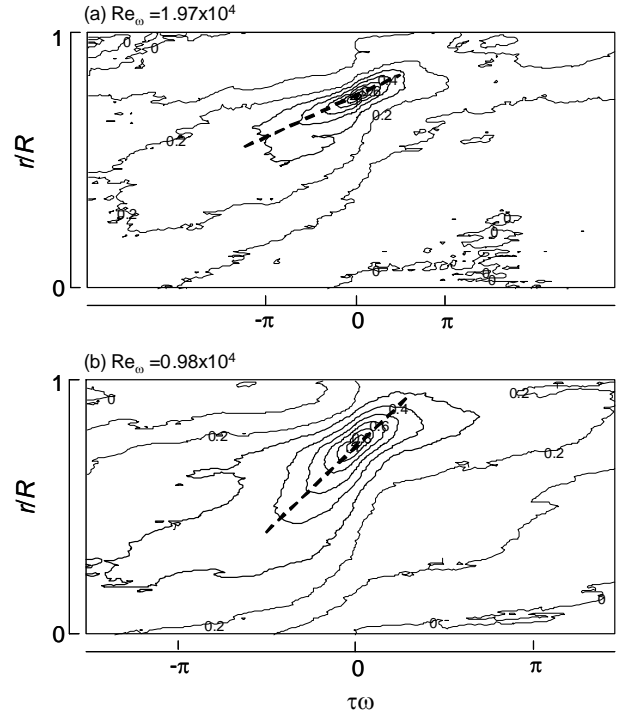

(a) $Re_\omega = 1.97 \times 10^4$

(b) $Re_\omega = 0.98 \times 10^4$

Fig.5 Contour maps of correlation coefficient of the reconstructed velocity fluctuation at Gr=1.84×10^8

Fig.6 Variation of integral scale

Fig.4 Reconstructed velocity field at $Re_\omega = 0.98 \times 10^4$, Gr=$1.84 \times 10^8$ corresponding to the Fig.3(c)
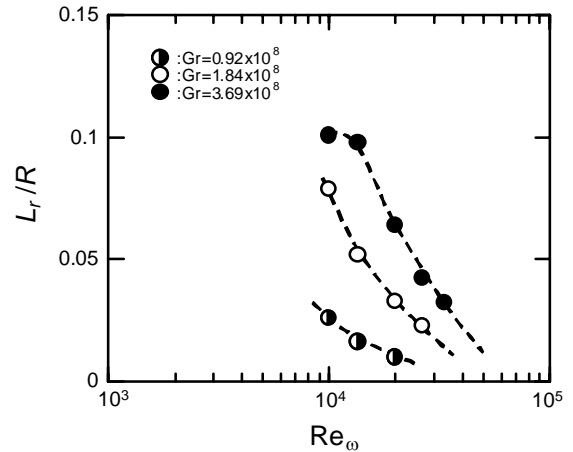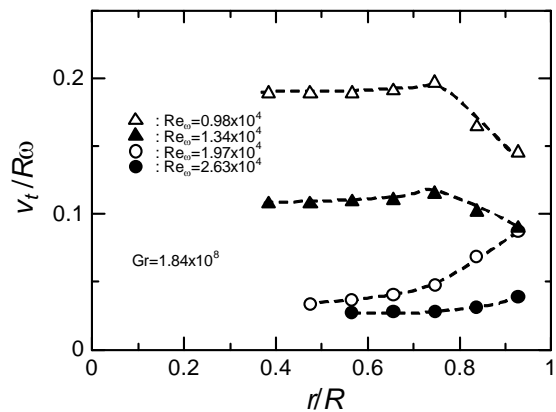

Fig.7 Radial variation of the traveling velocity of vortex

as shown by the dotted line, the traveling velocity decreases with increasing Reynolds number. An increase of the Reynolds number induces an increase of v_r component by the centrifugal force. However, in spite of this matter, the traveling velocity decreases with Reynolds number. This is also concerning with the conservation of the angular momentum.

Classification

To clarify the dominant region of each force from the view point of vortex appearance, we plot symbols in the Reynolds and Grashof number correlation as Fig.9 whether vortex can be observed or not. As shown by the hatching region, steady detection case as which a position of vortex appearance is stable, unsteady detection case as which is unstable and un-detection case is classified. The solid line indicated by Ogino et al.[5] is the critical Grashof number which classifies the dominant region of natural and forced convection. Their result was obtained by the variation of the Nuselt number on the heated rotating disk. They also suggested that the vortex can be observed well around this critical Grashof number. Our result is in good agreement with Ogino's for the steady detection case. The higher limitation as observed in the integral scales of Fig.6 and traveling velocity of Fig.8 is agreement with the critical Grashof number. On the other hand, for the unsteady detection case, the vortex can be observed at $Re_\omega > 0.986 \times 10^4$, $Gr > 0.922 \times 10^8$. The phenomena of these flow structure is typical one investigated under only mixed convection since the vortex can not be observed in other region dominated by the natural or forced convection.

The solid line by Ogino et al. is showing $Gr \sim Re_\omega^{3/2}$. They suggested the agreement with the linearity unsteady analysis by Wu and Cheng[6] in spite of the difference of the flow field. On the other hand, the dotted line is showing $Gr \sim Re_\omega^{5/2}$. When the flow direction between the convection and buoyancy is different, the dominant region by natural and forced convection is separated by this relationship obtained by a dimensional analysis[7]. For the unsteady detection case, the dotted line is in agreement with the limitation for detection of vortex. As concluding of result, the behavior on the heated rotating disk is classified to I to III region in the figure. The I is the region dominated by the forced convection induced by the rotating the disk. The III is by the buoyancy induced by the heating. The IIa and IIb is the mixed convection region which decided by the unstable flow structure on the heated rotating disk.

CONCLUDING REMARKS

The flow field on the heated rotating disk as the mixed convection condition was measured by the UVP. From the spatio-temporal velocity field, it was found that the vortex appears under typical condition and it travels to outside of the disk. The scale of the vortex decreases with Reynolds number and increases with Grashof number. The traveling velocity of the vortex also shows similar variation. According these result, the dominated region by natural, forced and mixed convection were classified.

REFERENCES

1. F. Kreith, J.H. Taylor, J.P.Chong, 1959, Heat and mass transfer form a rotating disk, *Trans. ASME J. of Heat Transfer*, 81, pp-95-105
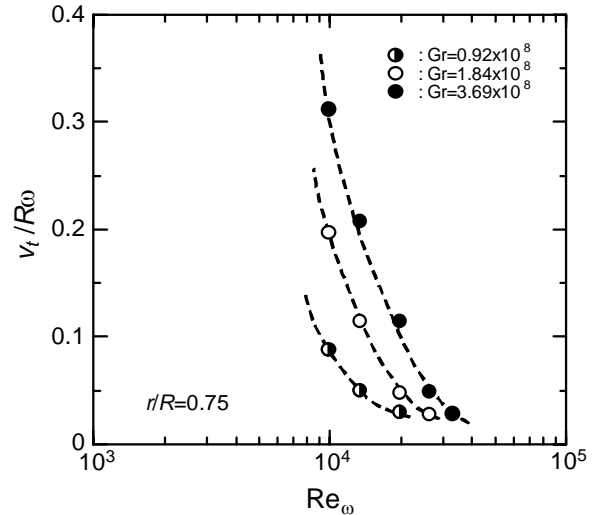
Fig.8 Variation of the traveling velocity of vortex
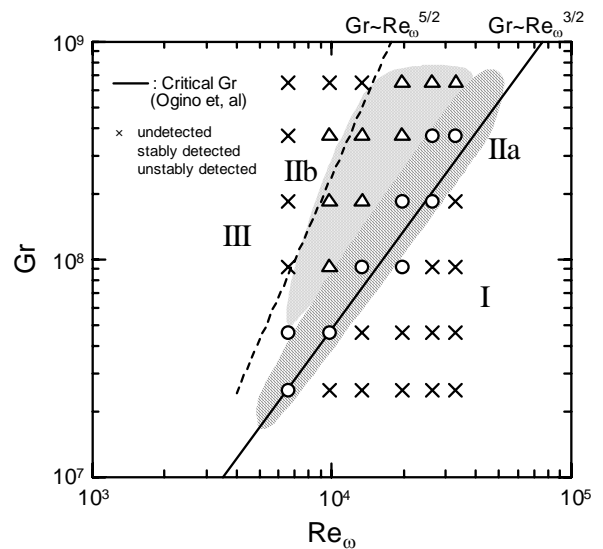

Fig.9 Detection of vortex

2. C.J Elkins, J.K. Eaton, 2000, Turbulent heat and momentum transport on a rotating disk, *J. of Fluid Mech.*, 402, pp.225-253

3. P. Jacobs, G.N. Ivey, 1998, The influence of rotation on shelf convection, *J. of Fluid Mech.*, 369, pp.23-48

4. U.R. Christensen, 2002, Zonal flow driven by strongly supercritical convection in rotating spherical shells, J. of Fluid Mech., 470, pp.115-133

5. F. Ogino, Y, Saitoh, T. Yoshida, K. Masuda, K. Mizuta, 1997, Heat tannsfer and flow characteristics in a rotating disk system, J. of Chemical Engineering of Japan, 23-5, pp.679-686 (in Japanese)

6. R.S. Wu, K.C. Cheng, 1976, Thermal instability of Blasius flow along horizontal plates, *Int. J. Heat Mass Transfer*, 19, pp.907-913

7. G. Wickern, 1991, Mixed convection from an arbitrarily inclined semi-infinite flat plate – I. The influence of the inclination angle, *Int. J. Heat and Mass Transfer*, 34, 8, pp.1935-1945